Cell. Mol. Biol. (ISSN: 1165-158X)

Journal Homepage: www.cellmolbiol.org

Cellular and Molecular Biology

Original Article

Comprehensive molecular analyses of a 7-m^{6}A-related lncRNAs signature for prognosis, tumor immunity and therapeutic effect in patients with hepatocellular carcinoma

Xiaomin Wu[1,#], Yi Wang[2,#], Leilei Tao[3], Yi Zhou[4], Xiaojing Zhang[5], Li Wang[1], Yingchun Zhang[1], Jun Jin[1], Jun Wang[1], Jinbiao Chen[1], Xiaomin Zhang[1], Xiankai Wang[1], Jixian Yu[1,*]

[1] Department of Oncology, Xixi Hospital of Hangzhou, Zhejiang University School of Medicine, Hangzhou, Zhejiang 310023, China
[2] Department of Institute of Hepatology and Epidemiology, Xixi Hospital of Hangzhou, Zhejiang University School of Medicine, Hangzhou, Zhejiang 310023, China
[3] Department of Oncology, Yancheng No.1 People's Hospital, Affiliated Hospital of Nanjing University Medical School, Yancheng, Jiangsu 224200, China
[4] Department of Nursing, Huashan Hospital, Fudan University, Shanghai 200000, China
[5] Department of Gynecologic Oncology, Zhejiang Cancer Hospital, Hangzhou, Zhejiang 315000, China

Article Info

Article history:

Received: November 29, 2023
Accepted: January 10, 2024
Published: January 31, 2024

Use your device to scan and read the article online

Abstract

Hepatocellular carcinoma is the most common form of liver tumor. m^{6}A modification and noncoding RNA show indispensable roles in HCC. We sought to establish and verify an appropriate m^{6}A-related long noncoding RNA prognostic tool for predicting hepatocellular carcinoma progression. We extracted the RNA expression levels and the clinicopathologic data from GTEx and TCGA databases. Multivariate Cox regression analysis and receiver operating characteristic curves were performed to test the model's predictive ability. We further built a nomogram for overall survival according to the risk score and clinical features. A competing endogenous RNA network and Gene Ontology assessment were implemented to identify related biological mechanisms and processes. By bioinformatics analysis, a risk model comprising GABPB1-AS1, AC025580.1, LINC01358, AC026356.1, AC009005.1, HCG15, and AC026368.1 was built to offer a prognostic prediction for hepatocellular carcinoma independently. The prognostic tool could better prognosticate hepatocellular carcinoma patients' survival than other clinical characteristics. Then, a nomogram with risk score and clinical characteristics was created, which had strong power to calculate the survival probability in hepatocellular carcinoma. The immune-associated processes involving the differentially expressed genes between the two subgroups were displayed. Analyses of prognosis, clinicopathological characteristics, tumor mutation burden, immune checkpoint molecules, and drug response showed significant differences among the two risk subtypes, hinting that the model could appraise the efficacy of immunotherapy and chemotherapy. The tool can independently predict the prognosis in patients with hepatocellular carcinoma, which benefits drug selection in hepatocellular carcinoma patients.

Keywords: Hepatocellular carcinoma; LncRNA; m^{6}A modification; Tumor mutational burden; Nomogram; Prognosis prediction

1. Introduction

Liver cancer comes sixth in respect of incidence and third in cancer-related mortality worldwide [1]. Hepatocellular carcinoma (HCC) comprises 75 to 85% of all pathological kinds of liver cancers. Chronic hepatitis B and C virus infection, heavy drinking, and metabolic abnormalities are the major risk factors for HCC [2]. Over the past decade or two, targeted therapy and immunotherapy have been used as primary systemic therapy for advanced HCC [3, 4]. Despite several advances in the treatment of HCC, the survival rate at 5 years after diagnosis is still low. Serum alpha-fetoprotein (AFP) is the most common biomarker of HCC. However, around half of patients with HCC are AFP-negative, especially early and small HCCs [5]. Hence, it is critical to determine more key biomolecules complementary to AFP for optimizing diagnostic accuracy and therapeutic decisions in HCC cases.

N6-methyladenosine (m^{6}A), one of the most prevalent RNA modifications, shows indispensable roles in diverse molecular processes, including transcription, processing, and metabolism [6]. RNA m^{6}A methylation is composed of methyltransferase ("Writer"), binding protein ("Reader"), and demethylase ("Erase"). Recent studies found a pivotal role of dysregulated m^{6}A modifications in various

* Corresponding author.
E-mail address: jixianyu0783@163.com (J. Yu).
# These authors contributed equally
Doi: http://dx.doi.org/10.14715/cmb/2024.70.1.25

types of cancer, including HCC [7-9]. For instance, upregulated YTHDF1 promotes the occurrence and development of breast cancer by enhancing tumor glycolysis [10]. In addition, KIAA1429 could facilitate the progression of tumor, which suggests it might be a novel oncogenic factor in colorectal cancer [11].

Long non-coding RNAs (lncRNAs) are a series of non-coding RNAs that contain more than 200 nucleotides, which regulate the expression of genes at the transcriptional and post-transcriptional levels [12]. The role of lncRNAs in promoting tumorigenesis and invasion has been well-documented in several cancers, including HCC [13]. Meanwhile, m^{6}A regulators could affect cancer development by changing the methylation level of lncRNA. However, the prognostic value of m^{6}A-related lncRNAs in HCC remains to be discovered.

In our work, we analyzed the RNA expression profile and clinical characteristics of HCC patients and established a risk signature that could effectively predict HCC progression. Then, we created a competing endogenous RNA (ceRNA) network for exploring underlying molecular mechanisms. Besides, we identified the potential compounds that might have therapeutic values in HCC. To summarize, our in-depth research identifies promising lncRNAs that can be positioned as prognostic biomarkers and provide better selections of the potential therapeutic target in HCC.

2. Materials and Methods

2.1. Preparation and Processing of Data

RNA expression matrix and clinical features of HCC patients were downloaded from the TCGA database (https://portal.gdc.cancer.gov/) and GTEx database (https://gtexportal.org/home/). HCC patients with missing survival data were removed from our study. Eventually, we filtered 13425 lncRNAs from the GTEx-TCGA database for the following analysis. Besides, 24 m^{6}A regulators were retrieved from the published research findings, comprising writers (WTAP, METTL3, METTL14, METTL16, VIRMA, RBM15, RBM15B, ZC3H13, and ZCCHC4), erasers (FTO and ALKBH5) and readers (YTHDC1, YTHDC2, YTHDF1, YTHDF2, YTHDF3, HNRNPC, HNRNPA2B1, FMR1, RBMX, LRPPRC, IGF2BP1, IGF2BP2, and IGF2BP3).

2.2. Acquisition of m^{6}A-related lncRNAs and Construction of Model

Pearson correlation analysis was developed to investigate the correlation between m^{6}A regulators and lncRNAs (|Pearson R| > 0.3 and P < 0.05). Afterwards, we selected differentially expressed mRNAs (DEmRNAs) and lncRNAs (DElncRNAs) utilizing the limma package (|log2FC| > 1 and FDR < 0.05). DElncRNAs and m^{6}A-associated lncRNAs were intersected to obtain differentially expressed m^{6}A-associated lncRNAs (DEMlncRNAs). Kaplan-Meier (K-M) and univariate Cox regression analyses were applied to select the prognostic DEMlncRNAs in the GTEx-TCGA database. LASSO (least absolute shrinkage and selection operator) regression was applied to determine the more dependent DEMlncRNAs by the glmnet R package. The 7 DEMlncRNAs were obtained from multivariate Cox regression analysis, after which we established an m^{6}A-related lncRNAs signature (MRLS). The risk score is computed using the following formula: Risk score = $\sum$(Exp[lncRNA]*Coef[lncRNA]). Exp(lncRNA) represents the expression levels of each selected lncRNA, and Coef(lncRNA) is the corresponding coefficient. 370 HCC patients were randomly classified into the training cohort (N = 186) and the testing cohort (N = 184) in nearly 1:1 ratio. Afterwards, we categorized HCC patients into high-risk and low-risk sets using the median risk score. Using the timeROC R package, the analysis of the 1-, 3-, and 5-year receiver operating characteristic (ROC) was used to assess the accuracy of the MRLS in the complete cohort.

2.3. Function Enrichment Analysis

We used |log2FC| $\geq$ 1 along with FDR < 0.05 to get the differentially expressed genes (DEGs) between the two risk subgroups. In addition, we executed Gene Ontology (GO) assessment to identify the biological procedures related to the m^{6}A-associated lncRNAs, and we computed single-sample Gene Set Enrichment Analysis (ssGSEA) scores that represented the immune status by the "GSVA" R package. Heatmap showed differences in immune functions between two risk subgroups.

2.4. Tumor Mutational Burden and Expression of Immune Checkpoint Genes

Tumor mutational burden (TMB) has been reported to be an indicator of immune response and tumor behavior, which was generated from the somatic mutation data of TCGA. Thus, we analyzed the common mutations by the "maftools" R package and calculated the TMB for each tumor sample. Furthermore, different expression levels of seven immune checkpoints between two risk subgroups were analyzed by box plot using limma and ggpubr R packages.

2.5. Prediction of Potential Compounds

To evaluate the chemotherapeutic drug sensitivity in HCC therapy, we computed the half-maximal inhibitory concentration (IC50) values of potential compounds using the ggpubr, ggplot2, pRRophetic and limma R packages.

2.6. Construction of Nomogram

Univariate and multivariate Cox regression analyses identified the independent prognostic factors in HCC. On the basis of these results, a nomogram comprising age, gender, grade, risk score, and stage was plotted to prognosticate the 1-, 3-, and 5-year overall survival (OS) rates of HCC patients. Moreover, a calibration chart was used to estimate the exactness of the nomogram. Principal component analysis (PCA) was created to compare different distributions among all genes, 24 m^{6}A regulators, 1419 m^{6}A-associated lncRNAs, and 7 m^{6}A-associated lncRNAs between the high and low-risk subgroups.

2.7. ceRNA network construction

To elucidate the regulatory relationship of m^{6}A-related lncRNAs, five of seven DEMlncRNAs were obtained to predict target miRNAs based on miRcode (http://www.mircode.org/) and Starbase (http://starbase.sysu.edu.cn/) databases. We used miRDB (http://www.mirdb.org/), miRTarbase (http://mirtarbase.mbc.nctu.edu.tw/), and TargetScan ((http://www.targetscan.org/) databases to search targeted regulation between miRNAs and mRNAs. Then, the intersection between DEmRNAs and target mRNAs was imported into the ceRNA network, which was visua-

lized with "Cytoscape" software (version 3.7.2) [14].

3. Results

3.1. Identification of m^{6}A-Related lncRNAs

A flowchart illustrating this research process is presented in Figure 1A. A total of 13,425 lncRNAs were screened out from TCGA and GTEx databases among 370 HCC samples and 160 normal liver samples. 1419 m^{6}A-related lncRNAs were extracted from co-expression networks of lncRNAs and m^{6}A regulators, as displayed in Figure 1B. Additionally, we obtained 1784 DEmRNAs and 1497 DElncRNAs in the GTEx-TCGA database, including 1035 downregulated DEmRNAs, 749 upregulated DEmRNAs, 486 downregulated DElncRNAs, and 1011 upregulated DElncRNAs respectively. Finally, 468 shared DEMlncRNAs were obtained for the following analysis.

3.2. Establishment and Validation of the MRLS

In the training cohort, 24 lncRNAs were identified via univariate Cox regression analysis and were linked to the OS of HCC patients (Figure 2A). Subsequently, we further determined 13 lncRNAs by LASSO regression analysis (Figure 2B, 2C). After applying the multivariate Cox regression analysis, 7 prognostic m^{6}A-related lncRNAs (GABPB1-AS1, AC025580.1, LINC01358, AC026356.1, AC009005.1, HCG15, and AC026368.1) were included as the prognostic signature. The correlation between m^{6}A regulatory genes and 7 m^{6}A-associated lncRNAs in the entire set is shown in Figure 1C. Risk score was calculated using the following formula: risk score = (-1.541 * GABPB1-AS1 exp.) + (0.760 * AC025580.1 exp.) + (0.715 * LINC01358 exp.) + (-2.640 * AC026368.1 exp.) + (1.459 * AC026356.1 exp.) + (0.442 * AC009005.1 exp.) + (0.801 * HCG15 exp.). HCC patients were classified into high/low-risk sets using the cutoff score. As shown in Figures 2D-2F, the risk score distribution, survival status, and expressions of 7 m^{6}A-associated lncRNAs in HCC patients were presented. K-M survival plot showed that patients with low-risk value had significantly longer OS than those with high-risk value ($P < 0.001$; Figure 2G). As we expected, a similar trend was verified in the testing and entire cohorts (Figures 2H-2K). In the three cohorts, we found statistically significant differences between the two risk subgroups respectively.

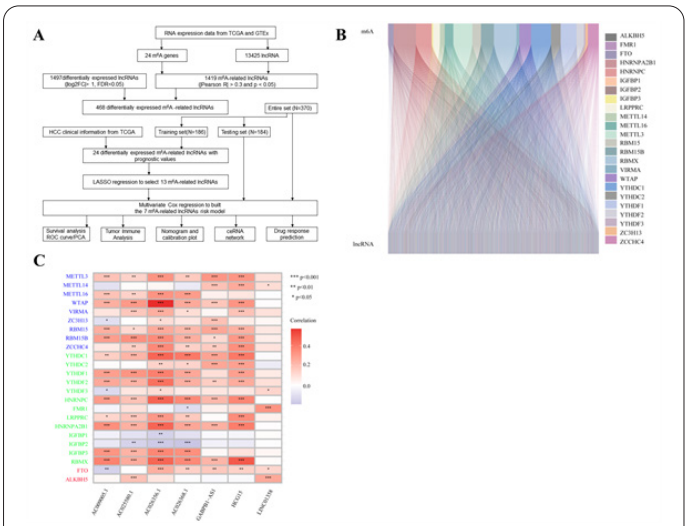

Fig. 1. The correlation between m^{6}A regulators and m^{6}A-related lncRNAs. (A) Flowchart for illustrating this research process. (B) Sankey relational diagram for 24 m^{6}A regulators and 1419 m^{6}A-related lncRNAs. (C) Pearson's correlation between 24 m^{6}A genes and 7 m^{6}A-related lncRNAs.

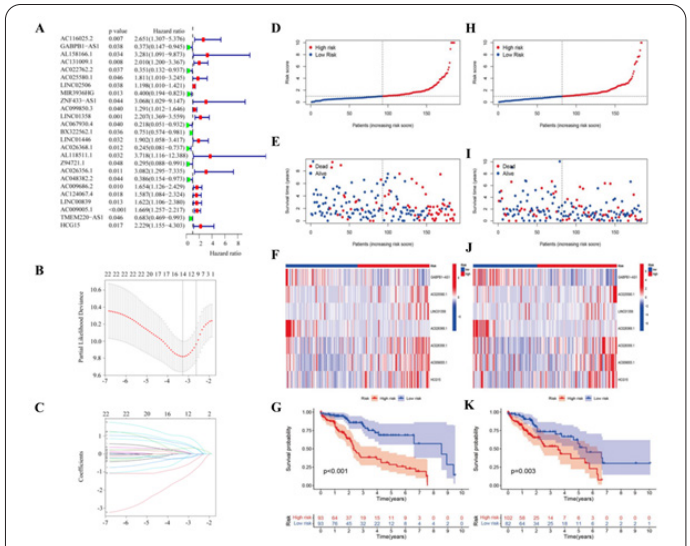

Fig. 2. Establishment of a m^{6}A-related lncRNAs risk model for HCC patients. (A) Univariate Cox regression analysis identified 24 lncRNAs. (B, C) LASSO regression was performed, calculating the minimum criteria. (D) Distribution of risk score. (E) Different patterns of survival status between the high/low-risk subgroups. (F) Heatmap of the 7 prognostic lncRNAs. (G) KM survival curves revealed that patients with low-risk scores had better overall survival than patients with high-risk scores. (H) Distribution of risk score for the testing cohort. (I) Patterns of the survival status between the high/low-risk subgroups for the testing cohort. (J) Heatmap of the 7 prognostic lncRNAs in the testing cohort. (K) KM curves showed a higher survival rate in the low-risk group for the testing cohort.

We also analyzed the correlation between the risk model and clinical features (Figure 3A-3H). The results demonstrated that high-risk HCC populations had shorter OS than low-risk populations, regardless of subgroups defined by age, gender, grade or stage. This situation also occurred in TNM Stage I-II subgroup, but there was no significant difference in Stage III-IV subgroup. It may be because the TCGA database included only five patients with stage IV.

Next, we implemented PCA to compare different distributions among entire expression genes, m^{6}A regulators, 1419 m^{6}A-related lncRNAs, and 7 m^{6}A-related lncRNAs between the two risk subgroups (Figures 3I-3L). These results indicated that 7 m^{6}A-associated lncRNAs had the best classification performance and could divide all samples into two risk sections quite well.

3.3. Tumor Immune Analysis and Tumor Mutational Burden

GO analysis was conducted to pick up the biological processes related to the MRLS. The results suggested that the DEGs between the two risk subgroups were closely correlated with immune-related biological processes, including humoral immune response and leukocyte-mediated immunity (Figure 4A). Using the ssGSEA method, we further discovered remarkable differences in the scores of immune functions among the two subgroups, such as MHC class I, APC_co stimulation, cytokine, and cytokine receptor (CCR), para-inflammation, checkpoint, T cell co-stimulation, inflammation-promoting, and HLA, suggesting that these immune functions are more active in high-risk

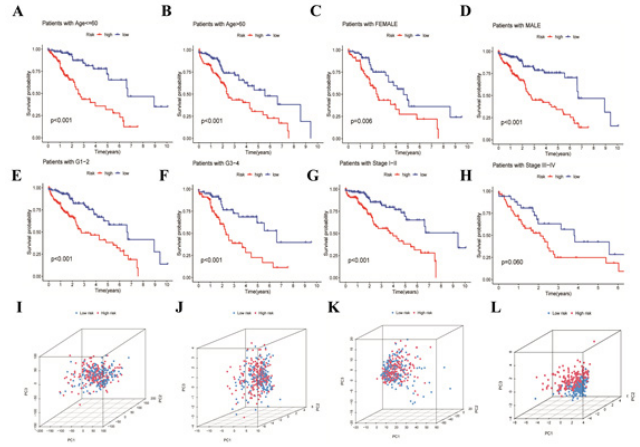

Fig. 3. Principal component analysis between the two risk subgroups. (A-H) KM curves of OS differences stratified by age, gender, tumor grade, or stage between the high/low-risk subgroups in the entire cohort. (I) all genes, (J) 24 m^{6}A genes, (K) 1419 m^{6}A-related lncRNAs, and (L) 7 m^{6}A-associated lncRNAs.

patients (Figure 4B). Furthermore, the difference analysis of tumor immune checkpoints (PDL1, B7H3, CTLA4, LAG3, TIM3, IDO1, and TIGIT) showed as follows: high-risk patients exhibited elevated expression levels of PDL1, B7H3, CTLA4, TIM3, IDO1, and TIGIT (Figures 4C-4H), while LAG3 expression was similar in two risk subgroups (Figure 4I).

As demonstrated in Figure 4J, high-risk patients displayed higher TMB compared to low-risk patients (P = 0.038). The alteration frequencies of TP53 and MUC16 were significantly higher in high-risk patients (Figures 4K, 4L). However, the alteration frequencies of CTNNB1 and ALB were markedly higher in low-risk patients. K-M curve indicated that the low-mutation set outperformed the high-mutation set in terms of OS (P = 0.006; Figure 4M). Subsequently, we explored the relationship between the MRLS and TMB, and the results revealed that patients in the high-TMB/high-risk group had a worse OS than patients in the low-TMB/low-risk group (P < 0.001; Figure 4N).

3.4. Differential response of treatments upon two risk cohorts

The pRRophetic algorithm was applied to figure out which drugs might affect HCC patients by looking at the IC50 of different drugs from the Genomics of Drug Sensitivity in Cancer (GDSC) database. The estimated IC50 levels of cisplatin (P = 0.0013; Figure 5A), gemcitabine (P = 0.0033; Figure 5B), and mitomycin C (P = 0.0015; Figure 5C) in the low-risk set were significantly higher than those in the high-risk set, and vinblastine (P =0.024; Figure 5D) had a lower IC50 level in the low-risk set than in the high-risk set. However, doxorubicin and sorafenib showed no significant difference (Figures 5E, 5F). Our findings demonstrated that high-risk populations were more responsive to cisplatin, gemcitabine, and mitomycin C, and low-risk populations were more responsive to vinblastine.

Univariate and multivariate Cox regression analysis revealed that MRLS and stage were both independent prognostic factors of HCC patients (Figures 5G, 5H). The ROC curves evaluated the predictive performance of the signature for 1, 3, and 5 years with area under curve (AUC) values of 0.701, 0.744, and 0.698, respectively, demonstrating that the model had good prediction efficiency (Figure 5I). Besides, the AUC of ROC curves, including risk model, age, gender, grade, and stage in entire group, were 0.701, 0.522, 0.527, 0.458, and 0.650, implying that the MRLS was reliable in predicting HCC patients' prognosis (Figure 5J). Furthermore, C-index analysis further manifested that risk score has better accuracy of prognostic prediction in HCC patients than other clinical features such as stage (Figure 5K).

We plotted a nomogram based on gender, age, grade, stage and risk score to calculate the 1-, 3-, and 5-year OS probabilities of HCC patients (Figure 5L). In addition, calibration plots confirmed good concordance between the prognostic outcome and actual observations (Figure 5M). All the results indicated that risk score might be a prediction tool to provide clinical guidance for HCC patients.

To further speculate on the potential mechanisms of m^{6}A-associated lncRNAs, we built a lncRNA-miRNA-mRNA ceRNA network. Five lncRNAs were selected from

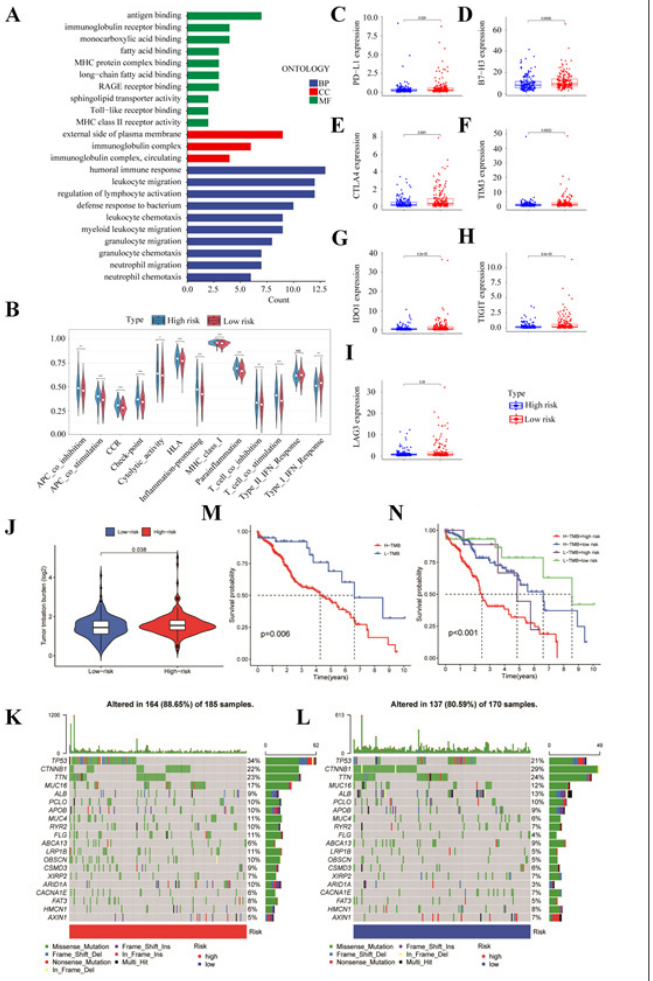

Fig. 4. Analysis of Tumor Immune and Tumor Mutational Burden using the m^{6}A-related lncRNA model in the entire set. (A) GO enrichment analysis. (B) Immune functions in the high-risk and low-risk groups. (C-I) The expression levels of PDL1, B7H3, CTLA4, TIM3, IDO1, TIGIT, and LAG3 in the high-risk and low-risk groups. (J) Correlation between risk score and TMB in two risk subgroups. (K) Gene mutation frequencies in the high-risk group. (L) Gene mutation frequencies in the low-risk group. (M) KM curves showed survival probability in high- and low-TMB patients. (N) KM curves showed OS in classified patients according to the m^{6}A-related lncRNA model and TMB.

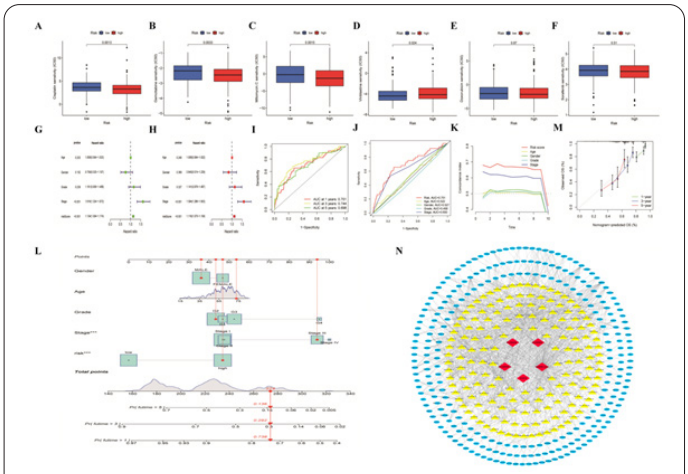

Fig. 5. Prediction of drug sensitivity in the high/low-risk subgroups and establishment of nomogram and performance evaluation. (A) Differences in cisplatin sensitivity in risk subgroups. (B) Differences in gemcitabine sensitivity in risk subgroups. (C) Differences in mitomycin C sensitivity in risk subgroups. (D) Differences in vinblastine sensitivity in risk subgroups. (E) Differences in doxorubicin sensitivity in risk subgroups. (F) Differences in sorafenib sensitivity in risk subgroups. (G) Univariate COX regression analysis shows that stage and risk score are related to the overall survival. (H) Multivariate COX regression analysis shows that stage and risk scores can be used as independent prognostic factors. (I) ROC curves of the risk score at 1, 3, and 5 years. (J) ROC curves of the clinical characteristics and risk score. (K) Concordance indexes of the clinical characteristics and risk score. (L) A nomogram for the risk score model and other clinicopathological factors in the entire cohort. (M) Calibration curves of the nomogram predict the probability of the 1-, 3-, and 5-year OS. (N) lncRNA-miRNA-mRNA ceRNA network generated by Cytoscape. Red: lncRNAs. Yellow: miRNAs. Blue: mRNAs.

seven m6A-related lncRNAs using the miRcode and starbase, and 313 target miRNAs were identified to interact with the five lncRNAs. Next, we selected 3109 mRNAs binding target miRNAs by miRTarbase, TargetScan, and miRDB. 256 mRNAs were filtered by incorporating the 3109 predicted mRNAs with 1,784 DEmRNAs in HCC patients. Finally, the ceRNA network was presented with Cytoscape software, involving 5 lncRNAs, 163 miRNAs, and 256 mRNAs (Figure 5N).

4. Discussion

HCC is a prevalent digestive system cancer with high incidence and mortality, which is often diagnosed at advanced stages owing to deficiency symptoms and signs [1]. Conversely, early detection, screening, and diagnosis of HCC ensures the availability of curative or effective treatments in most cases and improves patient prognosis [15]. The emerging biomarkers are unsatisfactory enough to be used for early surveillance of HCC. Therefore, exploring new molecular biomarkers and therapeutic targets to optimize HCC patient management is urgently needed.

It is widely recognized that RNA m⁶A modification occurs in several cellular processes, including cell metabolism, proliferation, migration, differentiation, and death [16]. The molecular mechanisms through which m⁶A regulators influence tumor progression and proliferation are multiple and involved in a variety of functions, including tumor stem cell formation, epithelial-mesenchymal transition (EMT), tumor metabolism, and cell signaling, by affecting the mRNA stability or protein translation [17]. Recent molecular studies, mainly directed towards RNA epigenetic alteration in cancers, have attempted to investigate the potential effects of m⁶A on cancer development and progression by detecting heterogeneity of m⁶A modification landscape and regulator expression levels. Several research studies have shown that deregulation of m⁶A is involved in many types of cancer by affecting the targeted mRNA or miRNA, as reviewed by Chen et al. [17]. However, current cancer studies regarding m⁶A modification in lncRNAs are scarce. Recently, Zuo et al. [18] demonstrated that METTL3-mediated m⁶A upregulates LINC00958 in HCC cells by regulating the stability of its transcript, thereby promoting the progression and lipogenesis of HCC. The m⁶A modification on Lnc-LSG1, which was regulated by METTL14, can prevent the interaction with ESRP2 via the m⁶A reader YTHDC1 in clear cell renal cell carcinoma [19]. LncRNA NEAT1, whose expression and m6A methylation level is significantly elevated by CRISPR/Cas13b-METTL3, can suppress the migration and progression of renal cell carcinoma [20]. These results are consistent with our hypothesis that m⁶A modification is closely related to lncRNAs. With these premises, we focused on the latent interplay between m6A modification and lncRNAs to reveal new prognostic indicators and precise treatment of HCC.

In this work, 7 m6A-related lncRNAs were used to develop the risk prediction model. The results of K-M analysis, ROC curves, and univariate and multivariate cox analysis have demonstrated that MRLS may be the more dependable clinical parameter. They will predict the OS of HCC patients independently. Among the above lncRNAs, two lncRNAs (GABPB1-AS1 and AC026368.1) expressions were positively correlated with OS, while five lncRNAs (AC025580.1, LINC01358, AC026356.1, AC009005.1, and HCG15) expression were negatively correlated with OS. The biological function of the vast majority of lncRNAs remains a mystery. HCG15 acted as a tumor-promoting factor in HCC cells by enhancing USF1-mediated ZNF641 transcription [21]. AC009005.1, a novel autophagy-related lncRNA, has been demonstrated as a predictor of prognosis in HCC patients [22]. GABPB1-AS1 triggered osteosarcoma development by targeting SP1 to activate the Wnt/β-catenin pathway [23]. Conversely, GABPB1-AS1, being involved in ferroptosis, functioned as a tumor suppressor and as an attractive therapeutic target for HCC [24]. The above studies confirmed that HCG15, AC009005.1 and GABPB1-AS1 are closely related to the progression of HCC, which further favors our findings. Notably, the role of lncRNAs AC026368.1, AC025580.1, LINC01358, and AC026356.1 was first reported and validated in our study. However, the regulatory mechanisms of these lncRNAs in tumors need to be further investigated.

We conducted a GO analysis to explore the DEGs between high/low-risk groups in HCC. Interestingly, we found that both immune response and immunoglobin occurred most frequently, implying that the immune microenvironment may be critical for HCC progression. Subsequently, the immune functions (MHC class I, CCR, checkpoint, T cell co-stimulation, APC co-stimulation, and HLA) were more active among the high-risk populations. Moreover, most of the immune checkpoint expressions were significantly up-regulated in high-risk HCC patients, implying that high-risk populations might respond better

to immunotherapy, which merited further validation in the future. A meta-analysis revealed that the poorer prognosis in HCC patients, along with elevated alpha-fetoprotein and poorly differentiated histology, is linked to the level of PD-L1 expression [25]. Analyses of other immune checkpoint expressions and their association with prognosis are awaited from numerous immunotherapy trials. Although anti-PD1/PDL1 and anti-CTLA4 monotherapies have been demonstrated to benefit patients with HCC [26-28], these trials achieve unsatisfactory response rates. This is likely due to the highly immunosuppressive state of the tumor microenvironment in the liver.

TMB, a promising biomarker, is the overall amount of somatic coding mutations, which links to the advent of neoantigens that induce antitumor immune responses [29]. The high TMB is a reliable predictor of clinical outcome and treatment response to immune checkpoint inhibitors in non-small-cell lung cancer [30, 31]. Xu found that patients with HCC harboring higher TMB have more effective immunotherapy responses and longer progression-free survival (PFS) than those with lower TMB [32]. The results of our article revealed that the high-risk set has higher TMB in comparison with the low-risk set. TMB has a strong relationship with the m^{6}A-related lncRNAs risk model. Additionally, the MRLS well-prognosticated mutation rates between high- and low-risk HCC cases, especially those of TP53, TTN, and CTNNB1 genes. High-risk populations had more increased TP53 mutations than low-risk cases (34% vs 21%). TP53 mutations impact the cell cycle in almost 30% of all HCC cases, and patients carrying this mutation tend to have unfavorable prognoses [2]. Interestingly, CTNNB1 was the highest mutated gene in the low-risk group. CTNNB1 mutations occurred in HCC lead to sparse T-cell infiltration and immune evasion through activating the β-catenin pathway [33, 34], implying that low-risk patients may have resistance to immunotherapy. People with higher TMB had worse OS than those with lower TMB. Therefore, these mutated genes and TMB may act as new targets for cancer therapy selection and monitoring and immune checkpoint biomarkers in combination with TMB should be used in the future to optimize therapeutic strategies for HCC patients.

Our study further explored the disparities in drug response between the two groups. Low-risk HCC patients were more sensitive to vinblastine. In contrast, high-risk patients were more susceptible to cisplatin, gemcitabine, and mitomycin C. As indicated above, the risk model might be helpful for guiding drug treatment choices. We then built a nomogram based on MRLS. Upon the completion of evaluation and verification, the risk model was suitable for prognosticating the prognosis of HCC. Finally, using the miRcode, starbase, miRTarBase, TargetScan, and miRDB databases, 5 lncRNAs, 163 miRNAs, and 256 mRNAs were identified to create their co-mediated ceRNA. Although we provided a comprehensive view of the underlying mechanism, further investigations are warranted to validate our findings.

Our study also has some limitations that need to be clarified. First, our signature was only validated using the GTEx-TCGA database without external data validation. Multi-center cohorts and other databases are required. Additionally, the functions of the identified lncRNAs have not been elucidated in depth. Further validation studies are needed to confirm the biological role of these lncRNAs in HCC.

5. Conclusion

Taken together, the MRLS can independently anticipate the prognosis in patients with HCC and optimize the treatment modalities. Besides, our study may contribute to explaining the primary process and mechanism of m6A-related lncRNAs.

Conflict of Interests

The author has no conflicts with any step of the article preparation.

Consent for publications

The author read and approved the final manuscript for publication.

Availability of data and material

The data that support the findings of this study are available from the corresponding author upon reasonable request.

Authors' contributions

XW and YW: Conceptualization, Methodology, Writing original draft. LT, YZ and XZ: Methodology, Investigation, Formal analysis, Validation. LW, YZ, JJ, JW and JC: Investigation, Formal analysis, Data curation. XZ and XW: Methodology, Validation, Writing review & editing, Supervision. JY: Writing review & editing, Supervision, Funding acquisition.

Funding

This work was supported by: Hangzhou Science and Technology Planning Projects (No. 20211231Y053).

Acknowledgments

We acknowledge the Cancer Genome Atlas and Genotype-Tissue Expression project for the clinicopathological and genetic alteration data.

References

1. Sung H, Ferlay J, Siegel RL, Laversanne M, Soerjomataram I, Jemal A, Bray F (2021) Global Cancer Statistics 2020: GLOBOCAN Estimates of Incidence and Mortality Worldwide for 36 Cancers in 185 Countries. CA Cancer J Clin 71 (3): 209-249. doi: 10.3322/caac.21660
2. Villanueva A (2019) Hepatocellular Carcinoma. N Engl J Med 380 (15): 1450-1462. doi: 10.1056/NEJMra1713263
3. Kudo M, Finn RS, Qin S, Han KH, Ikeda K, Piscaglia F, Baron A, Park JW, Han G, Jassem J, Blanc JF, Vogel A, Komov D, Evans TRJ, Lopez C, Dutcus C, Guo M, Saito K, Kraljevic S, Tamai T, Ren M, Cheng AL (2018) Lenvatinib versus sorafenib in first-line treatment of patients with unresectable hepatocellular carcinoma: a randomised phase 3 non-inferiority trial. Lancet 391 (10126): 1163-1173. doi: 10.1016/S0140-6736(18)30207-1
4. Sangro B, Sarobe P, Hervas-Stubbs S, Melero I (2021) Advances in immunotherapy for hepatocellular carcinoma. Nat Rev Gastroenterol Hepatol 18 (8): 525-543. doi: 10.1038/s41575-021-00438-0
5. Wang T, Zhang KH (2020) New Blood Biomarkers for the Diagnosis of AFP-Negative Hepatocellular Carcinoma. Front Oncol 10: 1316. doi: 10.3389/fonc.2020.01316
6. Chen XY, Zhang J, Zhu JS (2019) The role of m(6)A RNA methylation in human cancer. Mol Cancer 18 (1): 103. doi: 10.1186/

s12943-019-1033-z
7. Chen M, Wei L, Law CT, Tsang FH, Shen J, Cheng CL, Tsang LH, Ho DW, Chiu DK, Lee JM, Wong CC, Ng IO, Wong CM (2018) RNA N6-methyladenosine methyltransferase-like 3 promotes liver cancer progression through YTHDF2-dependent posttranscriptional silencing of SOCS2. Hepatology 67 (6): 2254-2270. doi: 10.1002/hep.29683
8. Lin X, Chai G, Wu Y, Li J, Chen F, Liu J, Luo G, Tauler J, Du J, Lin S, He C, Wang H (2019) RNA m(6)A methylation regulates the epithelial mesenchymal transition of cancer cells and translation of Snail. Nat Commun 10 (1): 2065. doi: 10.1038/s41467-019-09865-9
9. Sheng H, Li Z, Su S, Sun W, Zhang X, Li L, Li J, Liu S, Lu B, Zhang S, Shan C (2020) YTH domain family 2 promotes lung cancer cell growth by facilitating 6-phosphogluconate dehydrogenase mRNA translation. Carcinogenesis 41 (5): 541-550. doi: 10.1093/carcin/bgz152
10. Yao X, Li W, Li L, Li M, Zhao Y, Fang, Zeng X, Luo Z (2022) YTHDF1 upregulation mediates hypoxia-dependent breast cancer growth and metastasis through regulating PKM2 to affect glycolysis. Cell Death Dis 13 (3): 258. doi: 10.1038/s41419-022-04711-1
11. Zhou Y, Pei Z, Maimaiti A, Zheng L, Zhu Z, Tian M, Zhou Z, Tan F, Pei Q, Li Y, Liu W (2022) m(6)A methyltransferase KIAA1429 acts as an oncogenic factor in colorectal cancer by regulating SIRT1 in an m(6)A-dependent manner. Cell Death Discov 8 (1): 83. doi: 10.1038/s41420-022-00878-w
12. Grixti JM, Ayers D (2020) Long noncoding RNAs and their link to cancer. Noncoding RNA Res 5 (2): 77-82. doi: 10.1016/j.ncrna.2020.04.003
13. Samudh N, Shrilall C, Arbuthnot P, Bloom K, Ely A (2022) Diversity of Dysregulated Long Non-Coding RNAs in HBV-Related Hepatocellular Carcinoma. Front Immunol 13: 834650. doi: 10.3389/fimmu.2022.834650
14. Smoot ME, Ono K, Ruscheinski J, Wang PL, Ideker T (2011) Cytoscape 2.8: new features for data integration and network visualization. Bioinformatics 27 (3): 431-432. doi: 10.1093/bioinformatics/btq675
15. Wang W, Wei C (2020) Advances in the early diagnosis of hepatocellular carcinoma. Genes Dis 7 (3): 308-319. doi: 10.1016/j.gendis.2020.01.014
16. Wilkinson E, Cui YH, He YY (2022) Roles of RNA Modifications in Diverse Cellular Functions. Front Cell Dev Biol 10: 828683. doi: 10.3389/fcell.2022.828683
17. Chen M, Wong CM (2020) The emerging roles of N6-methyladenosine (m6A) deregulation in liver carcinogenesis. Mol Cancer 19 (1): 44. doi: 10.1186/s12943-020-01172-y
18. Zuo X, Chen Z, Gao W, Zhang Y, Wang J, Wang J, Cao M, Cai J, Wu J, Wang X (2020) M6A-mediated upregulation of LINC00958 increases lipogenesis and acts as a nanotherapeutic target in hepatocellular carcinoma. J Hematol Oncol 13 (1): 5. doi: 10.1186/s13045-019-0839-x
19. Shen D, Ding L, Lu Z, Wang R, Yu C, Wang H, Zheng Q, Wang X, Xu W, Yu H, Xu L, Wang M, Yu S, Zhu S, Qian J, Xia L, Li G (2022) METTL14-mediated Lnc-LSG1 m6A modification inhibits clear cell renal cell carcinoma metastasis via regulating ESRP2 ubiquitination. Mol Ther Nucleic Acids 27: 547-561. doi: 10.1016/j.omtn.2021.12.024
20. Chen J, Liao X, Cheng J, Su G, Yuan F, Zhang Z, Wu J, Mei H, Tan W (2021) Targeted Methylation of the LncRNA NEAT1 Suppresses Malignancy of Renal Cell Carcinoma. Front Cell Dev Biol 9: 777349. doi: 10.3389/fcell.2021.777349
21. Yan H, He N, He S (2022) HCG15 is a hypoxia-responsive lncRNA and facilitates hepatocellular carcinoma cell proliferation and invasion by enhancing ZNF641 transcription. Biochem Biophys Res Commun 608: 170-176. doi: 10.1016/j.bbrc.2022.03.143
22. Wu H, Liu T, Qi J, Qin C, Zhu Q (2020) Four Autophagy-Related lncRNAs Predict the Prognosis of HCC through Coexpression and ceRNA Mechanism. Biomed Res Int 2020: 3801748. doi: 10.1155/2020/3801748
23. Chen J, Bian M, Pan L, Liu C, Yang H (2022) GABPB1-AS1 Promotes the Development of Osteosarcoma by Targeting SP1 and Activating the Wnt/beta-Catenin Pathway. J Oncol 2022: 8468896. doi: 10.1155/2022/8468896
24. Qi W, Li Z, Xia L, Dai J, Zhang Q, Wu C, Xu S (2019) LncRNA GABPB1-AS1 and GABPB1 regulate oxidative stress during erastin-induced ferroptosis in HepG2 hepatocellular carcinoma cells. Sci Rep 9 (1): 16185. doi: 10.1038/s41598-019-52837-8
25. Li XS, Li JW, Li H, Jiang T (2020) Prognostic value of programmed cell death ligand 1 (PD-L1) for hepatocellular carcinoma: a meta-analysis. Biosci Rep 40 (4). doi: 10.1042/BSR20200459
26. El-Khoueiry AB, Sangro B, Yau T, Crocenzi TS, Kudo M, Hsu C, Kim TY, Choo SP, Trojan J, Welling THR, Meyer T, Kang YK, Yeo W, Chopra A, Anderson J, Dela Cruz C, Lang L, Neely J, Tang H, Dastani HB, Melero I (2017) Nivolumab in patients with advanced hepatocellular carcinoma (CheckMate 040): an open-label, non-comparative, phase 1/2 dose escalation and expansion trial. Lancet 389 (10088): 2492-2502. doi: 10.1016/S0140-6736(17)31046-2
27. Sangro B, Gomez-Martin C, de la Mata M, Inarrairaegui M, Garralda E, Barrera P, Riezu-Boj JI, Larrea E, Alfaro C, Sarobe P, Lasarte JJ, Perez-Gracia JL, Melero I, Prieto J (2013) A clinical trial of CTLA-4 blockade with tremelimumab in patients with hepatocellular carcinoma and chronic hepatitis C. J Hepatol 59 (1): 81-88. doi: 10.1016/j.jhep.2013.02.022
28. Zhu AX, Finn RS, Edeline J, Cattan S, Ogasawara S, Palmer D, Verslype C, Zagonel V, Fartoux L, Vogel A, Sarker D, Verset G, Chan SL, Knox J, Daniele B, Webber AL, Ebbinghaus SW, Ma J, Siegel AB, Cheng AL, Kudo M, investigators K- (2018) Pembrolizumab in patients with advanced hepatocellular carcinoma previously treated with sorafenib (KEYNOTE-224): a non-randomised, open-label phase 2 trial. Lancet Oncol 19 (7): 940-952. doi: 10.1016/S1470-2045(18)30351-6
29. Sha D, Jin Z, Budczies J, Kluck K, Stenzinger A, Sinicrope FA (2020) Tumor Mutational Burden as a Predictive Biomarker in Solid Tumors. Cancer Discov 10 (12): 1808-1825. doi: 10.1158/2159-8290.CD-20-0522
30. Alborelli I, Leonards K, Rothschild SI, Leuenberger LP, Savic Prince S, Mertz KD, Poechtrager S, Buess M, Zippelius A, Laubli H, Haegele J, Tolnay M, Bubendorf L, Quagliata L, Jermann P (2020) Tumor mutational burden assessed by targeted NGS predicts clinical benefit from immune checkpoint inhibitors in non-small cell lung cancer. J Pathol 250 (1): 19-29. doi: 10.1002/path.5344
31. Huang D, Zhang F, Tao H, Zhang S, Ma J, Wang J, Liu Z, Cui P, Chen S, Huang Z, Wu Z, Zhao L, Hu Y (2020) Tumor Mutation Burden as a Potential Biomarker for PD-1/PD-L1 Inhibition in Advanced Non-small Cell Lung Cancer. Target Oncol 15 (1): 93-100. doi: 10.1007/s11523-020-00703-3
32. Xu J, Zhang Y, Jia R, Yue C, Chang L, Liu R, Zhang G, Zhao C, Zhang Y, Chen C, Wang Y, Yi X, Hu Z, Zou J, Wang Q (2019) Anti-PD-1 Antibody SHR-1210 Combined with Apatinib for Advanced Hepatocellular Carcinoma, Gastric, or Esophagogastric Junction Cancer: An Open-label, Dose Escalation and Expansion Study. Clin Cancer Res 25 (2): 515-523. doi: 10.1158/1078-0432.CCR-18-2484
33. Berraondo P, Ochoa MC, Olivera I, Melero I (2019) Immune Desertic Landscapes in Hepatocellular Carcinoma Shaped by beta-Catenin Activation. Cancer Discov 9 (8): 1003-1005. doi:

10.1158/2159-8290.CD-19-0696

34. Montironi C, Castet F, Haber PK, Pinyol R, Torres-Martin M, Torrens L, Mesropian A, Wang H, Puigvehi M, Maeda M, Leow WQ, Harrod E, Taik P, Chinburen J, Taivanbaatar E, Chinbold E, Sole Arques M, Donovan M, Thung S, Neely J, Mazzaferro V, Anderson J, Roayaie S, Schwartz M, Villanueva A, Friedman SL, Uzilov A, Sia D, Llovet JM (2022) Inflamed and non-inflamed classes of HCC: a revised immunogenomic classification. Gut. doi: 10.1136/gutjnl-2021-325918